Nonequilibrium temperature and thermometry in heat-conducting ϕ^4 models

Wm. G. Hoover and Carol G. Hoover
Ruby Valley Research Institute, Highway Contract 60, Box 598 Ruby Valley, Nevada 89833, USA
(Received 20 January 2008)

We analyze temperature and thermometry for simple nonequilibrium heat-conducting models. We also show in detail, for both two- and three-dimensional systems, that the ideal-gas thermometer corresponds to the concept of a local instantaneous mechanical kinetic temperature. For the ϕ^4 models investigated here the mechanical temperature closely approximates the local thermodynamic equilibrium temperature. There is a significant difference between the kinetic temperature and nonlocal configurational temperature. Neither obeys the predictions of extended irreversible thermodynamics. Overall, we find that the kinetic temperature, as modeled and imposed by the Nosé-Hoover thermostats developed in 1984, provides the simplest means for simulating, analyzing, and understanding nonequilibrium heat flows.

DOI: XXXX PACS number(s): 05.20.−y, 05.45.−a, 05.70.Ln, 07.05.Tp

I. INTRODUCTION

The present work emphasizes and details the mechanical nature of the kinetic temperature, in contrast to the ensemble-based configurational temperature. Simulations for the simple models considered here are insensitive to system size and show significant differences between the kinetic and configurational temperatures. Our main goal is to illustrate and emphasize the relative advantages of the kinetic temperature, particularly away from equilibrium.

Ever since the early days of molecular dynamics, "temperature" has been based on the familiar ideal-gas kinetic-energy definition. For a Cartesian degree of freedom at equilibrium the kinetic definition is

$$kT_K \equiv \langle mv^2 \rangle .$$

This definition provides a means for linking Gibbs' and Boltzmann's classical statistical mechanics to thermodynamics. Because thermodynamic equilibrium corresponds to the Maxwell-Boltzmann velocity distribution,

$$f(v) = \sqrt{(m/2\pi kT)}\exp[-mv^2/2kT],$$

any of the even moments

$$\langle v^2 \rangle = 1 \times (kT/m),$$

$$\langle v^4 \rangle = 1 \times 3 \times (kT/m)^2,$$

$$\langle v^6 \rangle = 1 \times 3 \times 5 \times (kT/m)^3,$$

$$\ldots,$$

can be used to define the temperature for a system *at* equilibrium. The second-moment choice is not only the simplest, but in the ideal-gas case it also corresponds to a conserved quantity: the energy. The same definition of temperature is a fully consistent choice *away* from equilibrium too.

An *ideal-gas thermometer* can be visualized as a collection of many very small, light, and weakly interacting particles, but with such a high collision rate that thermal equilibrium (the Maxwell-Boltzmann distribution) is *always* maintained within the thermometer. For an innovative implementation of this model with molecular dynamics, see Ref. [1].

Configurational temperature definitions are also possible. There are two motivations for considering such coordinate-based temperatures: first, there is some ambiguity in determining the mean velocity in a transient inhomogeneous flow—the kinetic temperature has to be measured relative to the flow velocity while configurational temperature does not—second, the search for novelty. The simplest of the many configurational possibilities was suggested and also implemented by Jepps [2]. In independent research directed toward finding a canonical-ensemble dynamics consistent with configurational temperature, Travis and Braga developed an implementation identical to Jepps' unpublished algorithm [3]. The underlying expression for the configurational temperature,

$$kT_C \equiv \langle F^2 \rangle / \langle \nabla^2 \mathcal{H} \rangle ,$$

appeared over 50 years ago in Landau and Lifshitz' statistical physics textbook [4]. In the definition of kT_C the force F for a particular degree of freedom depends upon the corresponding gradient of the Hamiltonian:

$$F = -\nabla \mathcal{H} .$$

Landau and Lifshitz showed that the expression for kT_C follows from Gibbs' canonical distribution,

$$f_{\text{Gibbs}} \propto \exp[-\mathcal{H}/kT],$$

by carrying out a single integration by parts:

$$\langle \nabla^2 \mathcal{H} \rangle = \langle (\nabla \mathcal{H})^2 \rangle / kT \rightarrow kT_C \equiv \langle (\nabla \mathcal{H})^2 \rangle / \langle \nabla^2 \mathcal{H} \rangle .$$

Unlike the kinetic temperature, the configurational temperature T_C is not simply related to a mechanical thermometer. And in fact, there are *many* other such nonmechanical temperature expressions. Away from equilibrium it is clear that no finite number of moments or averages can be expected to uniquely define a phase-space distribution function. For a thorough discussion see Refs. [2] and [3]. Long before this complexity surfaced the proper definition of temperature away from equilibrium was a lively subject. To capture some of its flavor over a 30-year period see Refs. [5] and [6].

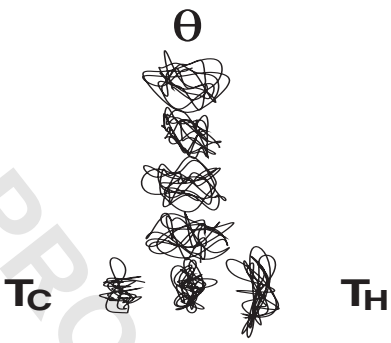

FIG. 1. Jou and co-worker's nonequilibrium system (described in detail in Sec. III), driven by the temperature difference $T_H - T_C$, is coupled to a thermometer which reads the "actual" or "correct" or "equilibrium" or "operational" temperature T_θ. This idea underlies our own simulations. Here T_θ represents temperature "at" the contact point between the vertical "thermometer" and the particle located between the two thermostated particles. Each of the seven particles in the system is represented here by a short trajectory fragment.

Relatively cumbersome microcanonical versions of the configurational temperature have been developed following Rugh's investigations. For references and an early application of these variants see Morriss and Rondoni's work [7].

Jou and co-workers and their critics [8–12] have considered the desirability of measuring an "operational" "thermodynamic" temperature for nonequilibrium systems. They discussed and then implemented a method [8,12] (which we explore in more detail here) for its measurement. Figure 1 illustrates the simplest case of their idea: a heat conductor connected to a "thermometer." As usual, the devil is in the details. Here the details include both the *type* of thermometer used and the linkage connecting that thermometer to the conducting system. The linkage certainly has an effect on the forces and internal energy at the linkage point, and hence affects the local-thermodynamic-equilibrium temperature and the configurational temperature. In addition to their "operational" temperature, Jou and co-workers also consider a "Langevin temperature" T_{Langevin} (the temperature which enters explicitly into the usual equilibrium Langevin equations of motion) and a "local thermodynamic equilibrium" temperature T_{LTE} (the temperature based on the equilibrium equation of state),

$$T_{\text{LTE}} \equiv T(\rho, e),$$

where e is the internal energy per unit mass). *At* equilibrium, and only at equilibrium, all of the various temperatures are the same and there is no ambiguity in the temperature concept:

$$T = T_K = T_C = T_{\text{Langevin}} = T_{\text{LTE}} \ [\text{at equilibrium}].$$

Away from equilibrium, where most physical interpretations of temperature are actually symmetric second-rank tensors, we can expect that each of the these four "temperatures" differs from the others. This *tensor* nature of temperature is evident in strong shock waves [13]. Generally we must anticipate that the nonequilibrium temperature can be anisotropic, with

$$T^{xx}_{K,C,\text{LTE}} \neq T^{yy}_{K,C,\text{LTE}} \neq T^{zz}_{K,C,\text{LTE}}.$$

This anisotropicity makes it imperative to describe the microscopic mechanics of any nonequilibrium thermometer in detail and argues strongly against a nonequilibrium version of the zeroth law of thermodynamics.

In their illustrative example, Hatano and Jou [12] used the temperature of a Langevin oscillator [14] coupled to a driven oscillator to measure the driven oscillator's temperature. A Langevin oscillator is damped with a constant friction coefficient and driven with a random force [14]. See also the next-to-last paragraph of Sec. II. Hatano and Jou [12] found that their measured temperature was qualitatively sensitive to the assumed form of coupling linking their "system" (the driven oscillator) to their "thermometer" (the Langevin oscillator).

At equilibrium, thermometry and thermodynamics, itself, both rely on the observation often called the zeroth law of thermodynamics, that two bodies in thermal equilibrium with a third are also in thermal equilibrium with each other (independent of the couplings linking the bodies). Hatano and Jou drew the very reasonable conclusion from their work that this fundamental property of temperature, which makes equilibrium thermometry possible, might be *impossible* away from equilibrium.

Baranyai [15,16] considered a much more complicated thermometer, a tiny crystallite, made up of a few hundred tightly bound miniparticles. He compared both the kinetic and configurational temperatures of nonequilibrium flows with the temperatures within his thermometer and found substantial differences. Baranyai was able to conclude from his work that neither the kinetic nor the configurational temperature was a "good" nonequilibrium temperature. By this, he meant that neither satisfied the zeroth law of thermodynamics. The temperature within Baranyai's minicrystal thermometer, his "operational temperature," exhibited relatively small spatial variations (the entire many-body thermometer was about the same size as a single particle of the nonequilibrium system in which it was immersed).

There is a considerable literature extending irreversible thermodynamics away from equilibrium, based on defining the nonequilibrium temperature, in terms of an (ill-defined) nonequilibrium entropy:

$$T = (\partial E / \partial S_{\text{noneq}})_V.$$

For a recent guide to the literature, see Ref. [17].

At equilibrium, Gibbs and Boltzmann showed that the entropy S_{eq} of a classical system is simply the averaged logarithm of the phase-space probability density:

$$S_{\text{eq}} = -k\langle \ln f_{\text{eq}} \rangle.$$

Away from equilibrium f_{noneq} is typically fractal [18,19] (so that its logarithm diverges), so that the very existence of a *nonequilibrium* entropy appears doubtful. For a comprehensive review of efforts based on a *nonequilibrium* Gibbs entropy, presumably $-k\langle \ln f_{\text{noneq}} \rangle$, see Ref. [20]. It is evident that such efforts are inconsistent with what is known about

the singular fractal nature of nonequilibrium phase-space distributions $\{f_{\text{noneq}}\}$.

Recent thorough work by Daivis [21] investigated the consequences of an *assumed* nonequilibrium entropy. Daivis compared three equalities (analogous to the equilibrium Maxwell relations) based on the assumed existence of S_{noneq} with results from numerical simulations. *None* of the three "equalities" was satisfied by the simulation results, casting doubt on both the existence of a nonequilibrium entropy analogous to the Gibbs-Boltzmann entropy and also on the existence of a corresponding entropy-based temperature.

In the present work we will explore these ideas for a simple nonequilibrium model of heat flow: the ϕ^4 model [19,22]. This very basic model has quadratic Hooke's-law interactions linking nearest-neighbor pairs of particles. In addition, each particle is tethered to its individual lattice site with a quartic potential. This model has been extremely useful for nonequilibrium statistical mechanics. In its most useful temperature range (where the particles are sufficiently localized, as detailed in Sec. IV) we will see that the internal energy varies nearly linearly with kinetic temperature, simplifying the analyses. The model obeys Fourier's law (for small enough temperature gradients for the equivalence of all the various temperature definitions), even in one dimension [22]. It can also display considerable phase-space dimensionality loss [19], establishing the fractal nature of the phase-space distribution function. Because the loss can exceed the phase-space dimensionality associated with the thermostating particles, a *fractal* distribution for the interior Newtonian part of a driven nonequilibrium system is implied by these results. We use the ϕ^4 model here to elucidate and compare the kinetic and configurational candidates for nonequilibrium temperature.

Though the mechanical models we consider are small, with only a few dozen degrees of freedom, we firmly believe that the analysis of such very specific manageable models is the only reliable guide to an understanding of thermometry and temperature. The pitfalls and complexities associated with large systems, and with large thermometers, are the gradients and inhomogeneities already seen in Baranyai's work [15,16].

The paper is organized as follows: first, a discussion of mechanical thermometry, using the ideal-gas thermometer, with simulations corresponding to ideal gases of disks (two dimensions) and spheres (three dimensions); next, a description of the computer experiment suggested by Jou as applied to the ϕ^4 model. After discussing and illustrating the ϕ^4 model, numerical results, and conclusions based on them, make up the final sections of this work.

II. IDEAL-GAS THERMOMETRY

Hoover, Holian, and Posch [9] described the mechanics of a one-dimensional ideal-gas thermometer in detail. They considered a massive particle, with momentum MV, interacting with a Maxwell-Boltzmann bath of ideal-gas particles with momenta $\{mv\}$. Here we will consider the same situation in detail for two- and three-dimensional thermometers. A typical collision can be viewed in the center-of-mass frame, a coordinate frame with the center-of-mass velocity

$$v_{\text{c.m.}} = \frac{MV + mv}{M + m}.$$

For an instantaneous hard-sphere impulsive collision the direction of the *relative* velocities in this frame, averaged over all possible collisions of the two velocities,

$$\{v_{\text{before}}\} = \pm (V - v),$$

is directed *randomly* after collision. This simplification leads to a systematic expansion [9] of the energy change of the massive particle in half-integral powers of the mass ratio m/M. To second order in $\sqrt{m/M}$,

$$-\langle (d/dt)(MV^2/2)\rangle \propto (MV^2/2) - \langle (mv^2/2)\rangle$$
$$= (MV^2/2) - (3kT_K/2),$$

where T_K is the ideal-gas kinetic temperature.

For the details of other models (soft spheres, square wells, etc.) of the interaction between the massive particle and an ideal-gas-thermometer heat bath, a solution of the corresponding Boltzmann equation would be required. Nevertheless, on physical grounds it is "obvious" that a massive particle with (above/below)-average energy will (lose or gain) energy, on the average, as a result of its collisions with the equilibrating bath,

$$\langle \dot{E} \rangle \sim \text{sgn}(\langle E \rangle_{\text{eq}} - E).$$

It is an interesting exercise in numerical kinetic theory to confirm this expectation in two and three dimensions. Consider first a hard disk with unit radius and mass M with unit velocity $V=(1,0)$. Scattering for disks is anisotropic. On the average a disk retains a memory of its original velocity in the center-of-mass frame. To model the interaction of a massive disk with a heat bath of unit-mass-point particles at kinetic temperature T_K requires choosing Maxwell-Boltzmann bath-particle velocities $\{v\}=\{v_x,v_y\}$ as well as an angle $0<\alpha<2\pi$ for each collision, which specifies the location of the colliding bath particle relative to the massive disk. See Fig. 2 for typical results. These were obtained by using a random number generator [23] to simulate the collisions.

The velocity changes of the disk, ΔV, and the bath particle, Δv, are as follows for a collision described by the angle α:

$$\Delta V = (V - v)(R - r)(\cos(\alpha), \sin(\alpha))[2m/(M + m)],$$

$$\Delta v = (v - V)(R - r)(\cos(\alpha), \sin(\alpha))[2M/(M + m)].$$

A sufficiently long series of velocity changes $\{\Delta V\}$, computed in this way, can be used to find the averaged hard-disk energy change shown in the figure.

Results for $m=1$, $M=100$, and 5×10^6 randomly-chosen hard-disk collisions for each ideal-gas temperature are shown in Fig. 2. In analyzing these simulations it is necessary to weight the summed-up contributions of all the observed collisions with the relative velocities corresponding to each collision c:

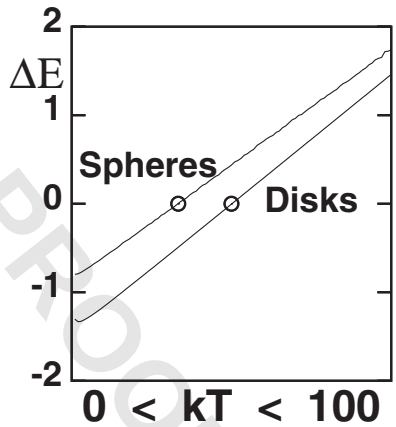

FIG. 2. Energy change, due to collisions, for a hard disk of mass M and unit speed with an equilibrium bath of point particles with mass $m=M/100$ and temperature T_K. Zero energy change corresponds precisely to that temperature (50 for disks, 33.333… for spheres, open circles in the figure) for which the disk kinetic energy equals the mean bath energy $\langle mv^2/k\rangle$. Also shown are analogous results for a hard sphere immersed in a hard-sphere ideal-gas thermometer.

$$\langle \Delta E\rangle = \frac{\sum (|v-V|\Delta E)_c}{\sum (|v-V|)_c}.$$

The speed $|v-V|$ is included because the collision rate for two randomly located particles with velocities v and V is directly proportional to the magnitude of their relative velocity, $v-V$.

As expected, the temperature at which the disk kinetic energy, for M equal to 100, is equal to the averaged mass-point thermal energy is 50:

$$\left\langle \Delta \frac{MV^2}{2} \right\rangle \propto 2kT_{\text{bath}} - MV^2.$$

The analogous averaged mass-point thermal energy is 33.333… for hard spheres. Energy changes for both disks and spheres are shown in Fig. 2. The simplicity of such a mechanical model for a thermometer—which "measures temperature" in terms of the kinetic energy per particle—recommends its use in analyzing nonequilibrium simulations.

The *configurational* temperature, on the other hand, has no corresponding mechanical model and also requires that the quotient of *two* separate averages be computed to find the temperature associated with a particular Cartesian degree of freedom:

$$kT_C \equiv \frac{\langle F^2\rangle}{\langle \nabla^2 \mathcal{H}\rangle}.$$

Kinetic temperature is simpler, requiring only a single average because $\nabla_p^2 \mathcal{H} = 1/m$ is constant:

$$kT_K \equiv \langle (\nabla_p \mathcal{H})^2\rangle / \langle (\nabla_p^2 \mathcal{H})\rangle = \langle p^2\rangle/m = m\langle v^2\rangle.$$

Unlike the kinetic temperature the configurational temperature is nonlocal (through its dependence on forces).

It should be noted that the "Langevin thermometer," as implemented by Hatano and Jou [12], *appears* to be based on a similar application of kinetic theory. But the Langevin thermometer, if viewed as a "thermostat" designed to impose the temperature T_{Langevin}, suffers from the defect that its "temperature" (given by the ratio of the time-integrated correlation function of the fluctuating force to the drag coefficient) is *not* equal to $\langle mv^2/k\rangle$ (or to any other oscillator-based temperature) except *at* equilibrium. The ideal-gas thermometer, on the other hand, maintains its temperature both at and away from equilibrium, and can easily be implemented in numerical simulations by using either Gaussian (constant kinetic energy) or Nosé-Hoover (specified time-averaged kinetic energy) mechanics. Both these thermostats employ feedback forces to maintain the specified kinetic temperature T_K even away from equilibrium.

Baranyai's thermometer [15,16], with hundreds of degrees of freedom, contains within it both stress and temperature gradients. His minicrystal thermometer translates, rotates, and vibrates as well. This complexity destroys the local instantaneous nature of temperature that is so valuable for analyzing inhomogeneous systems with large gradients.

III. JOU AND CO-WORKER'S THERMOMETRIC EXPERIMENT

In order to explore the concept of nonequilibrium temperature, Jou and Casas-Vázquez suggested [8], and Hatano and Jou ultimately tested [12], the setup shown in Fig. 1. As indicated in that figure, an equilibrium thermometer measures the "real," or "thermodynamic," or "operational" temperature T_θ when it is connected to a nonequilibrium system with a temperature intermediate to T_{hot} and T_{cold}. The constraint on individual particles' velocities imposed by the heat current in the nonequilibrium system suggests that the nonequilibrium temperature T_θ will turn out to be lower than the local thermodynamic equilibrium temperature T_{LTE} (the temperature based on mass, momentum, and energy through the equilibrium equation of state) [8,11]. "Extended irreversible thermodynamics" [17] provides an estimate for this temperature difference:

$$T_{\text{LTE}} - T_\theta \simeq Q^2,$$

where Q is the heat flux and the proportionality constant in this relation is a temperature- and-density-dependent material property. Although Hatano and Jou [12] confirmed that the kinetic temperature for a simple two-oscillator model actually *is* less than the temperature measured by a Langevin thermometer, the configurational temperature for this same model behaved oppositely, *exceeding* the Langevin temperature. This discrepancy led Hatano and Jou to conclude that the zeroth law of thermodynamics is unlikely to be obeyed away from equilibrium, once again shedding doubt on the existence of a nonequilibrium entropy.

In the present work we implement an extension of the Hatano and Jou simulation to a two-dimensional few-body system based on the ϕ^4 model [19,22], as described in the following section.

FIG. 3. Particle trajectories for 20 000 time steps. The cold particle kinetic temperature $T_K^{\rm cold}=0.01$ and the hot particle kinetic temperature $T_K^{\rm hot}=0.03$ are constrained with Nosé-Hoover friction coefficients. The corresponding measured configurational temperatures are 0.0159 and 0.0265. The long-time-averaged kinetic and configurational temperatures of the five Newtonian particles are (from bottom to top) {0.0207,0.0237,0.0238,0.0238,0.0242} and {0.0218,0.0229,0.0229,0.0229,0.0234}, respectively. See Table II. The heat flux is 0.002 69.

IV. ϕ^4 MODEL FOR NONEQUILIBRIUM THERMOMETRY

We consider a simple heat-conducting nonequilibrium system in two space dimensions. See Fig. 3 for a time exposure of the corresponding dynamics. There is a cold particle obeying the Nosé-Hoover equations of motion

$$\dot{x} = (p_x/m), \quad \dot{y} = (p_y/m),$$

$$\dot{p}_x = F_x - \zeta_{\rm cold} p_x, \quad \dot{p}_y = F_y - \zeta_{\rm cold} p_y,$$

$$\dot{\zeta}_{\rm cold} \propto (p_x^2 + p_y^2 - 2mkT_{\rm cold}).$$

Both the cold particle and an analogous hot particle (with $\zeta_{\rm hot}$ and $T_{\rm hot}$) are connected to a Newtonian particle with quadratic nearest-neighbor Hooke's-law bonds:

$$\phi_{\rm Hooke} = \frac{\kappa_2}{2}(r-d)^2.$$

See again Fig. 3.

The Newtonian particle through which the flux Q flows, from the hot particle to the cold one on the average, lies at the end of a chain of similar Newtonian particles. This chain of Newtonian particles acts as a *thermometer* through which no heat flows.

To validate the chain idea we carried out preliminary *equilibrium* simulations, with the "hot" and "cold" particles thermostated at a common temperature: $T_K^c = T_K^h = 0.07$. Simulations with 10^9 time steps (beginning after first discarding 0.5×10^9 equilibration time steps) were carried out for 7-, 14-, and 21-particle systems. These three simulations each provided time-averaged configurational and kinetic temperatures for *all* particles lying in the range $(0.0698 < T < 0.0701)$. These simulations indicated consistent equilibration along the chains and between the configurational and kinetic temperatures within a reasonable tolerance of ± 0.0001. We conclude from these equilibration runs that the ϕ^4 model is a sufficiently mixing and conducting system for use in *nonequilibrium* thermometry simulations.

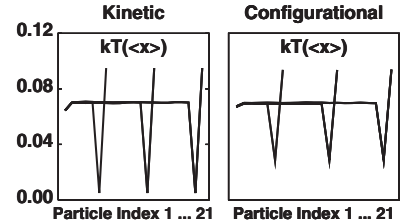

FIG. 4. Long-time-averaged temperature profiles for nonequilibrium systems of $n=\{7,14,21\}$ particles. Nosé-Hoover kinetic constraints control the kinetic temperatures of a "cold" particle, with $T_K^c=0.005$, Particle $n-1$, and a "hot" particle, with $T_K^h=0.095$, Particle n. Particle 1 lies between the "cold" particle and the "hot" particle. Both the kinetic and the configurational temperatures are shown for all n particles. These simulations used 1×10^9 time steps after discarding an equilibration run of 0.5×10^9 time steps. $dt=0.005$.

This convincing equilibration suggests that a *chain* of ϕ^4 particles *is* a suitable thermometer. How long should the chain be away from equilibrium? To find this out we next carried out an exactly similar series of three *nonequilibrium* simulations with an extreme factor-of-19 difference between the constrained cold and hot kinetic temperatures:

$$T_K^c = 0.005, \quad T_K^h = 0.095.$$

The long-time-averaged temperature results for 7-, 14-, and 21-particle systems, shown in Fig. 4, are essentially the same, so that a simple 4-particle chain of thermometric particles is sufficient.

Each of the particles in this nonequilibrium system is tethered to its lattice site r_0 with a quartic potential:

$$\phi_{\rm tether} = \frac{\kappa_4}{4}(r-r_0)^4.$$

With 7 particles there are 30 ordinary differential equations to solve (14 coordinates, 14 momenta, and 2 friction coefficients). For convenience we choose all of the particle masses, Boltzmann's constant k, the force constants κ_2 and κ_4, the Hooke's-law equilibrium spacing d, and the cold and hot proportionality constants determining the Nosé-Hoover friction coefficients, all equal to unity. For the cold particle we solve the following equations:

$$\dot{x} = p_x, \quad \dot{y} = p_y,$$

$$\dot{p}_x = F_x - \zeta_{\rm cold} p_x, \quad \dot{p}_y = F_y - \zeta_{\rm cold} p_y,$$

$$\dot{\zeta}_{\rm cold} = (p_x^2 + p_y^2 - 2T_{\rm cold}).$$

We have carried out many other simulations, using configurational or one configurational and one kinetic thermostat, as well as different particle numbers, but the results are qualitatively similar to those obtained with kinetic thermostats and are therefore not reported here. Likewise we do not explicitly consider here the possibility of separately thermostating the x and y directions (by using two friction coefficients ζ_T^{xx} and ζ_T^{yy}).

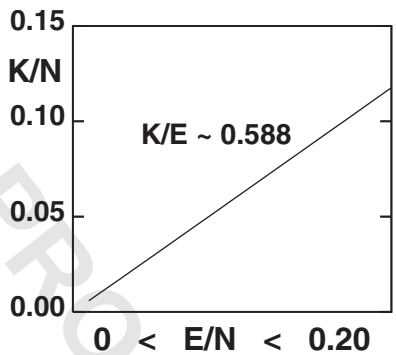

FIG. 5. Variation of kinetic energy with total energy for a 100-particle ϕ^4 chain at equilibrium. For each of the 20 points which the line connects here 10^7 time steps were used after discarding 5×10^6 equilibration time steps. $dt=0.005$. To an excellent approximation, $K\simeq0.588E$.

It should be noted that the Hooke's-law nearest-neighbor potential leads to *discontinuous forces* whenever particle trajectories *cross* one another. This is a common occurrence in either one or two dimensions, at sufficiently high temperatures. In one or two dimensions the force changes from ±1 to ∓1 as two particles pass through one another. To avoid (or at least minimize) these discontinuities in the present two-dimensional simulations we have only considered simulations with average temperatures less than or equal to 0.1.

In discussing the applicability of irreversible thermodynamics to nonequilibrium systems several workers have suggested the use of a "local thermodynamic equilibrium" temperature [5,8,11,17,20,24]. For the present model the relation between the local thermodynamic equilibrium temperature and the kinetic temperature is nearly linear. Figure 5 shows the variation of kinetic energy with internal energy for a periodic chain of 100 particles (results for 7- and 14-particle chains are essentially the same). To an accuracy better than a percent,

$$T_K \propto T_{\mathrm{LTE}}.$$

V. NUMERICAL RESULTS AND CONCLUDING REMARKS

Exploratory simulations of the type illustrated in Figs. 3 and 4 suggested that the kinetic and configurational temperatures are a bit different (away from equilibrium) and also that these temperatures vary slightly along the length of the Newtonian thermometric chain. At the same time the heat flow between the hot and cold particles closely follows Fourier's law. To show this explicitly Table I gives the kinetic and configurational temperatures for an average temperature $T^{\mathrm{av}}=(T^c+T^h)/2=0.05$ and a broad range of temperature differences $\Delta T=T^h-T^c$.

The tabulated results for temperature differences which are not too large,

$$\Delta T/T^{\mathrm{av}} < 1,$$

show a relatively small variation of the effective thermal conductivity for the three-particle (cold-Newton-hot) system,

TABLE I. Averages for runs of length $t=5\,000\,000$ with the fourth-order Runge-Kutta time step $dt=0.005$. The kinetic and configurational temperatures are listed, along with the heat flux Q (all accurate to the last figure). The first seven columns correspond to the temperatures of the cold and hot particles, followed by the temperature of the Newtonian particles (the Newtonian particles are the five shown in a vertical column in Fig. 3 and labeled from bottom to top).

T_K^c	T_K^h	T_K^1	T_K^2	T_K^3	T_K^4	T_K^5	Q
0.045	0.055	0.0504	0.0507	0.0507	0.0507	0.0507	0.0020
0.040	0.060	0.0512	0.0524	0.0526	0.0526	0.0528	0.0039
0.035	0.065	0.0526	0.0554	0.0558	0.0559	0.0560	0.0057
0.030	0.070	0.0542	0.0588	0.0593	0.0594	0.0595	0.0076
0.025	0.075	0.0559	0.0622	0.0628	0.0629	0.0631	0.0094
0.020	0.080	0.0574	0.0648	0.0655	0.0657	0.0659	0.0113
0.015	0.085	0.0588	0.0671	0.0678	0.0682	0.0681	0.0132
0.010	0.090	0.0603	0.0681	0.0689	0.0692	0.0690	0.0146
0.005	0.095	0.0643	0.0698	0.0706	0.0710	0.0707	0.0143
T_C^c	T_C^h	T_C^1	T_C^2	T_C^3	T_C^4	T_C^5	Q
0.0471	0.0537	0.0506	0.0506	0.0506	0.0506	0.0506	0.0020
0.0445	0.0578	0.0519	0.0522	0.0523	0.0522	0.0524	0.0039
0.0423	0.0623	0.0540	0.0548	0.0550	0.0550	0.0552	0.0057
0.0400	0.0672	0.0563	0.0578	0.0581	0.0581	0.0583	0.0076
0.0378	0.0723	0.0587	0.0608	0.0611	0.0610	0.0614	0.0094
0.0353	0.0775	0.0606	0.0631	0.0635	0.0635	0.0638	0.0113
0.0327	0.0831	0.0624	0.0655	0.0659	0.0659	0.0660	0.0132
0.0298	0.0886	0.0638	0.0669	0.0671	0.0670	0.0671	0.0146
0.0285	0.0937	0.0670	0.0694	0.0695	0.0695	0.0693	0.0143

TABLE II. Kinetic temperatures (above) and configurational temperatures (below) are shown as functions of the long-time-averaged (1×10^9 time steps) heat flux Q induced by the temperature difference $T_K^h - T_K^c$ between two thermostated Nosé-Hoover particles. The first seven columns correspond to the temperatures of the cold and hot particles, followed by the temperature of the Newtonian particles (the Newtonian particles are the five shown in a vertical column in Fig. 3 and labeled from bottom to top).

T_K^c	T_K^h	T_K^1	T_K^2	T_K^3	T_K^4	T_K^5	Q
0.001	0.003	0.00134	0.00146	0.00146	0.00146	0.00147	0.00002
0.002	0.006	0.0029	0.0031	0.0031	0.0031	0.0031	0.00008
0.005	0.015	0.0089	0.0100	0.0100	0.0100	0.0101	0.00064
0.010	0.030	0.0207	0.0237	0.0238	0.0238	0.0242	0.00269
0.020	0.060	0.0447	0.0504	0.0508	0.0508	0.0509	0.00736
0.050	0.150	0.1066	0.1132	0.1142	0.1148	0.1152	0.01858
T_C^c	T_C^h	T_C^1	T_C^2	T_C^3	T_C^4	T_C^5	Q
0.00125	0.00217	0.00135	0.00142	0.00140	0.00142	0.00145	0.00002
0.0025	0.0043	0.0029	0.0030	0.0030	0.0030	0.0031	0.00008
0.0075	0.0120	0.0095	0.0098	0.0097	0.0097	0.0099	0.00064
0.0159	0.0265	0.0218	0.0229	0.0229	0.0229	0.0234	0.00269
0.0311	0.0570	0.0470	0.0490	0.0492	0.0491	0.0494	0.00736
0.0673	0.1497	0.1104	0.1125	0.1133	0.1136	0.1138	0.01858

$$\kappa = 2Q/(T_K^h - T_K^c),$$

with the imposed temperature gradient. There are significant differences between the (local) kinetic and (nonlocal) configurational temperatures of the two thermostated particles. Similarly, the kinetic and configurational temperatures of the Newtonian particle linking them also differ somewhat. On the other hand, the near proportionality of the internal energy and the kinetic energy *at equilibrium* implies that local-thermodynamic-equilibrium temperature profiles and kinetic temperature profiles are essentially the same.

In every case the difference between the temperature of the Newtonian particle *with* a heat flux (particle 1) and the temperatures of the thermometric Newtonian particles without a heat flux (particles $2,\ldots,5$) is rather small, but significant. This difference is explored systematically in Table II, where a relatively large kinetic temperature difference

$$T_K^h = 3T_K^c \rightarrow \Delta T/T^{\mathrm{av}} = 1$$

is imposed. Symmetry suggests that the temperature difference should depend quadratically on the heat flux (this same dependence is also predicted by "extended irreversible thermodynamics" [8–11,17,20,24]). These simple arguments are wrong. In fact, the data in Table II suggest a square-root rather than a quadratic dependence. Figure 6 shows the dependence of the temperature differences $T_K^5 - T_K^1$ and $T_C^5 - T_C^1$ on the heat flux Q.

The data in both tables, calculated with all the Hooke's-law force constants equal to unity, are consistent with the set of *nonequilibrium* inequalities

$$T_\theta > T_C > T_K,$$

where T_θ is the thermometric temperature of the Newtonian thermometer while T_C and T_K are the configurational and kinetic temperatures of the Newtonian particle through which heat flows. On the other hand, simply reducing the force constant (from 1.0 to 0.3) linking that Newtonian particle to the thermometric chain (and leaving all the other force constants unchanged) gives *different* inequalities

$$T_C > T_\theta > T_K.$$

Whether or not the conducting Newtonian particle is "hotter" or "colder" than the thermometric chain depends on the definition of temperature *at* that particle. The anistropicity of the Newtonian particle's temperature is relatively small in these simulations and tends to decrease as the force constant linking that particle to the thermometric chain is decreased. For instance, $T_K^{yy} - T_K^{xx}$ is reduced from 0.012 to 0.006 as the linking force constant is reduced from 1.0 to 0.1. The sign of this disparity, $T_K^{yy} > T_K^{xx}$, is nicely consistent with the intuitive reasoning of Jou and Casas-Vázquez [8,11].

Evidently the predictions of extended irreversible thermodynamics are not particularly useful in understanding the temperature differences which result from small-system thermometry with relatively large thermal gradients. The detailed

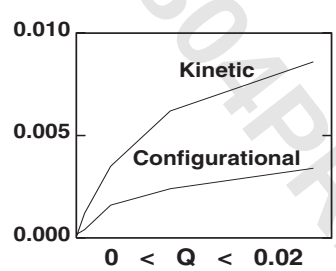

FIG. 6. Variation of the kinetic-temperature and configurational-temperature differences with heat flux, using the data from Table II. A *quadratic* variation in this plot (rather than the apparent *square root*) corresponds to the "predictions" of extended irreversible thermodynamics.

results depend upon the details of the thermometric linkage. Note that the configurational temperature of the hot (cold) thermostated particle lies *below* (*above*) the kinetic temperature, a symptom of the configurational temperatures' nonlocality. Because the *sign* of $T_K - T_C$ can vary, both mechanical and thermodynamical effects are involved.

In order to show that the qualitative features of thermometry for the ϕ^4 model are insensitive to temperature, we collect typical results in Table II for sets of cold and hot temperatures varying over two orders of magnitude. In each case the kinetic temperatures of the cold and hot particles are imposed by Nosé-Hoover thermostats. Then the long-time-averaged temperatures, both kinetic and configurational, are measured for all of the particles. The averaged heat flux is included too. The configurational temperature of the "cold" particle is uniformly higher than its kinetic temperature, while the configurational temperature of the "hot" particle is uniformly lower. This complexity is due to the nonlocal character of configurational temperature.

In summary, let us reiterate our findings. First, numerical kinetic theory simulations (Fig. 2) demonstrate the local instantaneous dynamical basis of kinetic temperature. Next, stationary heat flows demonstrate an insensitivity of the nonequilibrium temperature to system size (Fig. 4) and also show that the kinetic and configurational temperatures shift away from equilibrium can differ by more than a factor of 2. This disparity occurs despite the near equivalence (Fig. 5) of the kinetic temperature to the local-thermodynamic equilibrium temperature. Although it is possible to imagine and compute many "temperatures" away from equilibrium, none of which satisfies a zeroth law, we see no reason to prefer any definition more complicated than that of the ideal-gas thermometer. A mechanical, local, and instantaneous physical thermometer (which also corresponds well to a local thermodynamic equilibrium thermometer in the present case) is appealing. It is the simplest choice.

A particularly interesting problem where locality is important for nonequilibrium thermometry is the stationary shock-wave. There the differences between the longitudinal and transverse kinetic temperatures are extremely large (as measured by an ideal-gas thermometer) and the relaxation times are determined by the atomic vibration frequency rather than diffusive processes [13]. The extreme spatial gradients associated with strong shock waves make the smoothing associated with configurational temperature undesirable.

ACKNOWLEDGMENTS

Peter Daivis, Leopoldo García-Colín, Janka Petravic, Ian Snook, Billy Todd, Karl Travis, and Paco Uribe all made comments and suggestions as this work progressed. Karl Travis', Peter Daivis', and Janka Petravic's generous suggestions and corrections were specially useful. Billy Todd's kind invitation to visit Melbourne for MM2007 and Ian's hospitality at the Royal Melbourne Institute of Technology made this work possible. We thank one of the referees for pointing out that the concept of nonequilibrium temperature, emphasizing anisotropicity, is exhaustively reviewed in [25].

[1] M. Grünwald and C. Dellago, Mol. Phys. **104**, 3709 (2006).
[2] O. G. Jepps, Ph.D. thesis, Australian National University, Canberra, 2001.
[3] C. Braga and K. P. Travis, J. Chem. Phys. **123**, 134101 (2005).
[4] L. D. Landau and E. M. Lifshitz, *Statistical Physics* (Muir, Moscow, 1951) (in Russian), Eq. 33.14.
[5] L. S. García-Colín and M. S. Green, Phys. Rev. **150**, 153 (1966).
[6] B. C. Eu and L. S. García-Colín, Phys. Rev. E **54**, 2501 (1996).
[7] G. P. Morriss and L. Rondoni, Phys. Rev. E **59**, R5 (1999).
[8] D. Jou and J. Casas-Vázquez, Phys. Rev. A **45**, 8371 (1992).
[9] W. G. Hoover, B. L. Holian, and H. A. Posch, Phys. Rev. E **48**, 3196 (1993).
[10] K. Henjes, Phys. Rev. E **48**, 3199 (1993).
[11] D. Jou and J. Casas-Vázquez, Phys. Rev. E **48**, 3201 (1993).
[12] T. Hatano and D. Jou, Phys. Rev. E **67**, 026121 (2003).
[13] B. L. Holian, W. G. Hoover, B. Moran, and G. K. Straub, Phys. Rev. A **22**, 2798 (1980).
[14] I. Snook, *The Langevin and Generalised Langevin Approach to the Dynamics of Atomic, Polymeric, and Colloidal Systems* (Elsevier, Amsterdam, 2006).
[15] A. Baranyai, Phys. Rev. E **61**, R3306 (2000).
[16] A. Baranyai, Phys. Rev. E **62**, 5989 (2000).
[17] D. Jou, J. Casas-Vázquez, and G. Lebon, *Extended Irreversible Thermodynamics*, 3rd ed. (Springer, Berlin, 2001).
[18] Wm. G. Hoover, *Time Reversibility, Computer Simulation, and Chaos* (World Scientific, Singapore, 2001), p. 154.
[19] Wm. G. Hoover, K. Aoki, C. G. Hoover, and S. V. De Groot, Physica D **187**, 253 (2004).
[20] Á. R. Vasconcellos, J. G. Ramos, and R. Luzzi, Braz. J. Phys. **35**, 689 (2005).
[21] P. J. Daivis, J. Non-Newtonian Fluid Mech. (to be published).
[22] K. Aoki and D. Kusnezov, Phys. Lett. A **309**, 377 (2003).
[23] W. G. Hoover, *Computational Statistical Mechanics* (Elsevier, New York, 1991), p. 81.
[24] L. S. García-Colín and V. Micenmacher, Mol. Phys. **88**, 399 (1996).
[25] J. Casas-Vázquez and D. Jou, Rep. Prog. Phys. **66**, 1937 (2003).